Abdelaziz BOUCHIKHI

University of Saïda, Faculty of the Technology, Department of the Electrical Engineering, 20000, Algeria

doi:10.15199/48.2016.06.30

2D Fluid Approaches of a DC Normal Glow Discharge: Current Densities

Abstract. *In this manuscript, both electric and energy behavior of a 2D spatial distributions in the Cartesian geometry of electron, ion and total longitudinal current densities as well as both ionization and energy sources terms of a DC glow discharge in the normal mode and in low gas pressure are presented for the first time in the literature. The model used in this work is the second order fluid model (continuity and momentum transfer equations and energy equation for electrons). The set of equations are coupled in a self-consistent way with Poisson's equation. The results obtained in the stationary state are in good agreement with those given by literature.*

Streszczenie. *Analizowany jest prąd wyładowania DC i określany jest przestrzenny rozkład strumienia elektronów, jonów, prądu a także pokreślone są źródła energii jonizacji. Jako model do analizy przyjęto model płynu drugiego rzędu. Równania są sprzężone z odpowiednimi równaniami Poissona.* ***Model cieczy 2D do analizy wyładowania DC – gęstości prądów.***

Keywords: Normal glow discharge; Boltzmann's equation; Poisson's equation; electron diffusivity Einstein's relation
Słowa kluczowe: wyładowanie DC, równania Boltzmanna, równania Poissona

Introduction

DC glow discharges are widely used in the microelectronics industry as a source of reactive species for plasma etching or deposition (see e.g. Refs. [1-3]). A better understanding of these discharges and the ability to predict their properties for different operating conditions are a prerequisite for a better control of the process. Modeling of the discharges helps towards an understanding of their physical details and assists in optimizing their applications.

In this manuscript, the model is based on the local average energy approximation. The all physic average sizes depend on the local average energy of the particles. On the other hand, the distribution function is completely determined by both density and local average energy of electron or ion. This approach was adapted by Schmitt *et al.* [4], Belenguer and Bœuf [5], Oh *et al.* [6] and Bouchikhi *et al.* [7-9] in a one-dimensional geometry, who use the first three moments of the Boltzmann equation and suppose that the distribution function is Maxwellian for electrons. The simplification assumes in the moments of the Boltzmann equation was as follows:

1) The drift energy is negligible compared to the thermal energy.

2) The kinetic pressure tensor is diagonal and isotropy.

3) The average collision frequency depends on the local average energy.

4) The term ($\partial / \partial t$) in the movement quantity transfer equation is negligible compared with source term (in which intervene the frequency of exchange movement quantity ν_m).

5) An ionization coefficient is calculated with a Maxwellian distribution.

6) The secondary electron emission from the cathode is caused by the impact of positive ions

These assumptions also are used in the work of Bouchikhi *et al*. [10, 11] in a two-dimensional geometry. The authors have studied the DC glow discharge in the Subnormal mode [10] and in the normal mode [11]; we have been presented the 2D spatial distributions of electron and ion densities, both longitudinal and transversal electric field as well as electron temperature.

There are many problems for numerical simulation of current density in a 2D geometry. Therefore, this manuscript is concerned to represent the 2D spatial distributions of electron, ion and total longitudinal current densities, as well as, both ionization and energy sources terms. Since, it is rare to find such distributions in literature. On the other hand, these distributions are necessary to numerical simulations then for optimizing the reactor of plasma.

The outline of the manuscript is as follows. The model is briefly introduced and the initial boundary conditions, as well as numerical technique are described. The results obtained are shown, discussed and validated. Finally, concluding remarks are presented.

Discharge model

Under the continuum assumptions, which were cited previously, the set of governing equations are as follows:
Continuity equations for electron and ion:

(1) $$\frac{\partial n_e}{\partial t} + \nabla \mathbf{\Phi}_\mathbf{e} = S \ ,$$

(2) $$\frac{\partial n_i}{\partial t} + \nabla \mathbf{\Phi}_\mathbf{i} = S \ .$$

Momentum transfer equations [12, 13] for the electrons and positive ions are:

(3) $$\mathbf{\Phi}_\mathbf{e} = -\mu_e n_e \mathbf{E} - \nabla D_e n_e \ ,$$

(4) $$\mathbf{\Phi}_\mathbf{i} = \mu_i n_i \mathbf{E} - \nabla D_i n_i \ ,$$

(5) $$S = K_i N n_e \exp(-E_i / K_B T_e) \ ,$$

The relation between the electric field and the space charge in the inter-electrode space is given by Poisson's equation:

(6) $$\nabla E = \frac{|e|}{\varepsilon_0}\left(n_i - n_e\right) .$$

The electric field **E** is related to the potential by the following relation:

(7) $$E = -\nabla V \ .$$

The EINSTEIN'S relation is:

(8) $$D_e = \frac{\mu_e K_B T_e}{|e|} \ .$$

The equations for the electron energies are [10, 11]:

(9) $$\frac{\partial n_e \varepsilon_e}{\partial t} + \frac{5}{3}\nabla \mathbf{\Phi}_\varepsilon = S_\varepsilon \ ,$$

(10) $$\mathbf{\Phi}_\varepsilon = -\mu_e n_e \varepsilon_e \mathbf{E} - \nabla D_e n_e \varepsilon_e \ ,$$

(11) $$S_\varepsilon = -e\phi_{e_L} E_L - e\phi_{e_T} E_T - K_i N n_e \exp(-E_i / K_B T_e) H_i ,$$

and:

- ϕ_{e_L} is the longitudinal electron flux along the X axis
- ϕ_{e_T} is the transversal electron flux along the Y axis

$$E_L = -\frac{\partial V}{\partial x} \quad ; \quad E_T = -\frac{\partial V}{\partial y} .$$

- E_L is the longitudinal electric field along the X axis
- E_T is the transversal electric field along the Y axis

The transport coefficients for an argon gas have been taken from Lin *et al.* [14-16]. The inter-electrodes spacing is L=3.525 (cm). The electrode radius is R=5.08 (cm). Neutral species density is N=2.83 x 10^{16} (cm^{-3}); gas temperature is 323 (K); ion diffusivity is $D_i=10^2$ (cm^2s^{-1}); both electron and ion mobility are $\mu_e=2 \times 10^5$ ($cm^2v^{-1}s^{-1}$) and $\mu_i=2 \times 10^3$ ($cm^2v^{-1}s^{-1}$); ionization rate prefactor is $K_i=2.5 \times 10^{-6}$ (cm^3s^{-1}); ionization rate activation energy is E_i=24 (eV) and ionization enthalpy loss is H_i =15.578 (eV).

Initial and boundary conditions

The boundary conditions are required at each electrode and the initial conditions in order to complete the problem. The potential at the anode (x=0, y) is fixed to be zero (Volt) and at the cathode (x=L, y) equal to -77.4 (Volts). The secondary electron emission coefficient at the cathode is taken to be 0.046. The electron temperature at the cathode is 0.5 (eV).

The initial distributions of the electron and ion densities are set as a Gaussian form [17] given by the following relation:

(12) $$n_e = n_i = 10^7 + 10^9 (1-x/L)^2 (x/L)^2 + (1-y/2R)^2 (y/2R)^2 \ \mathrm{cm}^{-3}$$

The initial distribution of the electron temperature is chosen to be 1 eV.

The boundary conditions are set as follows:

- The electron density is equal to zero at the anode
- The electron and ion densities are taken as zero at the dielectric walls [18]
- The electric potential is in accordance with the Neumann condition ($\frac{\partial V}{\partial y} = 0$) at the dielectric walls

The effect of the secondary electron emission coefficient γ enters through the pertaining boundary conditions

(13) $$\phi_e\left(\frac{X}{L} = 1, y\right) = -\gamma \phi_i\left(\frac{X}{L} = 1, y\right) .$$

With L is the inter-electrode spacing

Numerical technique

The spatial discretization scheme used for the transport equations is the Scharfetter-Gummel [19] exponential scheme. This discretization is carried out in the Cartesian geometry. The transport equations of charged particles (electrons and ions) and Poisson's equation of them are solved using an implicit technique with a typical integration time step of the order of 10^{-9}s. Then, the resolutions of the equations set are solved by Thomas algorithm combined with the iterative relaxation method. The calculations were carried out on a Pentium 4 (3 GHz) personal computer. It took typically 24 hours and 30 minutes of run time to reach the converged solution for one set of discharge conditions.

Results and discussion

In this section, the results are given for the DC normal glow discharge in low pressure argon gas between plane-parallel electrodes. Two-dimensional distributions of the longitudinal current densities and both ionization and energy sources terms are presented to illustrate the discharge behavior.

Figs. 1, 2 and 3 represent the 2D spatial distributions and the contour plots of the longitudinal current densities of electron and ion and total in the stationary state of the normal glow discharge, respectively.

I observe that the distributions of the longitudinal current densities of electron, ion and total are more important at the symmetry axis of the electrodes (corresponding for y=0 (cm) of the electrode width). I notice, that the current densities of electron, ion and total decrease linear towards dielectric walls because of the boundary conditions that are imposed. The electron current density (see Figure 1) in the anodic region is larger than the current density in the cathode region; it is of order -1.8 x 10^{-3} $mAcm^{-2}$ in the anodic region at the symmetric axis of the electrodes. The longitudinal electron current density cannot be null in the cathode sheath because of the secondary electron emission coefficient process that is presence, which has caused by bombardment positive ions cathode surface from the ionized gas.

I also notice that the longitudinal ion current density (see Fig. 2) in the cathode region is larger than the current density in the anodic region due to the propagation of ions positive towards electrode cathode. It is about 1.8 x 10^{-3} $mAcm^{-2}$ in the cathode region at the symmetric axis of the electrodes. I observe there are accumulations of charged particle species of both ions in the anodic sheath region and of electrons in the cathode sheath. I notice that the longitudinal electron current density in the anodic sheath has the same value just like ion species in the cathode sheath, which has an almost symmetric behavior between the current densities of ion and electron species. Consequently, the longitudinal total current density (see Fig. 3) is almost constant in the inter-electrodes spacing (it has an average value which is 1.8 x 10^{-3} $mAcm^{-2}$ at the symmetric axis of the electrodes) and decreases on the dielectric walls' direction.

Fig. 4 illustrates the 2D spatial distributions and the contour plots of the ionization source term in the stationary state. It depends exponentially of electron temperature but varies linearly with electron density. The ionization source term is characterized in the discharge by two peak values; the first one in the sheath cathode and the second one in the negative glow. These two values with abscissas are S=1.3762 X 10^{13} ($cm^{-3}s^{-1}$) for X/L=0.7931 and S=5.0773 X 10^{12} ($cm^{-3}s^{-1}$) for X/L=0.6724 at the symmetric axis of the electrodes. The electron temperature influences directly on the ionization source term in both regions; the cathode sheath, and dielectric walls because of the electron density that is less significant. Fig. 5 represents the 2D spatial distributions and the contour plots of the energy source term in the stationary state. It is composed of three terms in the 2D geometry. Two terms are due to the heating, the first one of these two terms is generated by longitudinal electric field with longitudinal electron flux, and the second one is generated by transversal electric field with transversal electron flux. The third term is due to the cooling effect of electron species, it is generated by ionization process.

I notice that the energy source term has a symmetric value because of the physical phenomena's equilibrium which is in progress (cooling and heating). The heating effect due to the transversal electric field is perceptible on the dielectric walls.

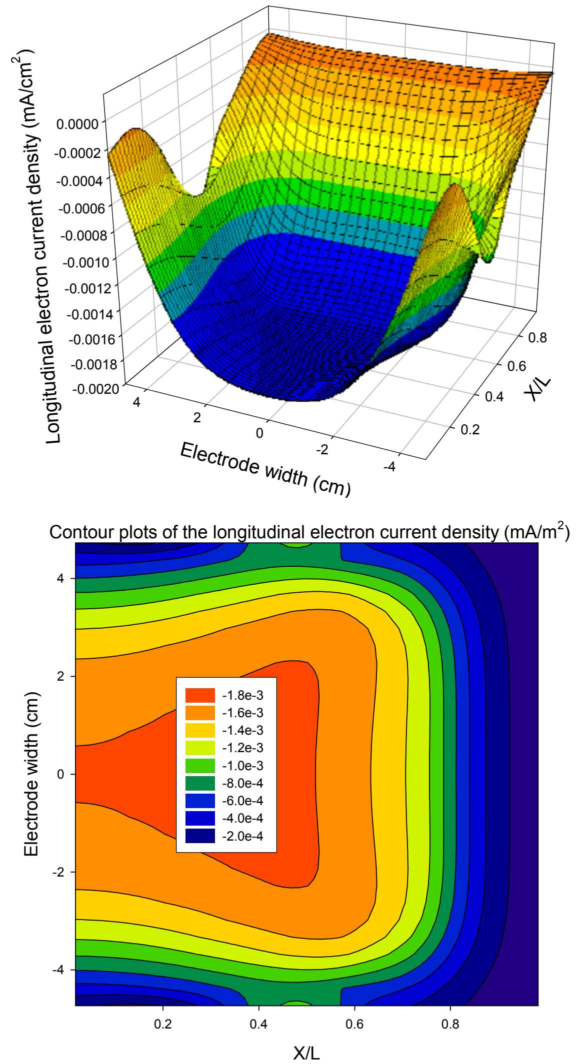

Fig. 1. Presentation in 2D and in contour plots of the longitudinal current density of electron in the stationary state

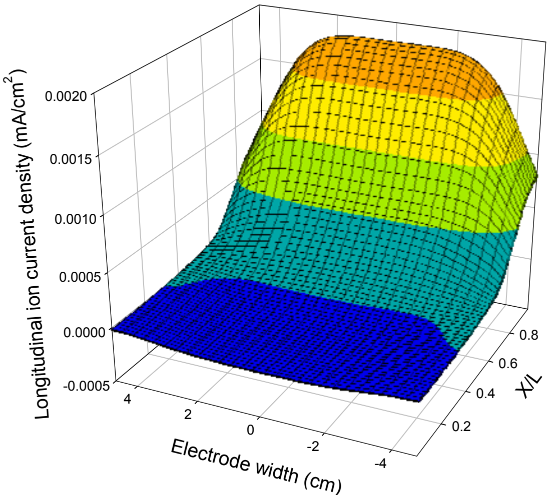

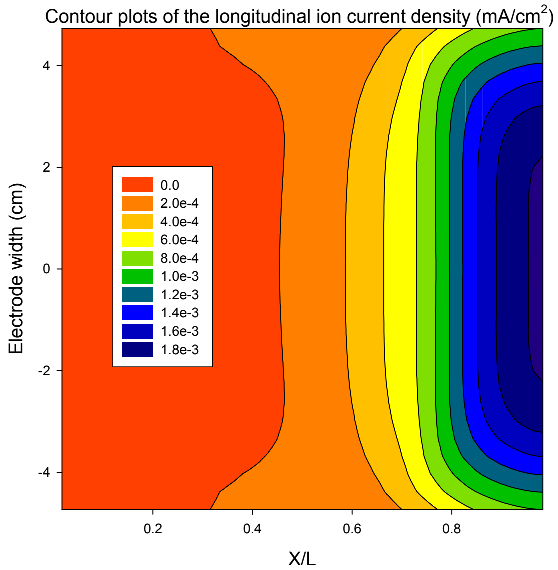

Fig. 2. Presentation in 2D and in contour plots of the longitudinal current density of ion in the stationary state.

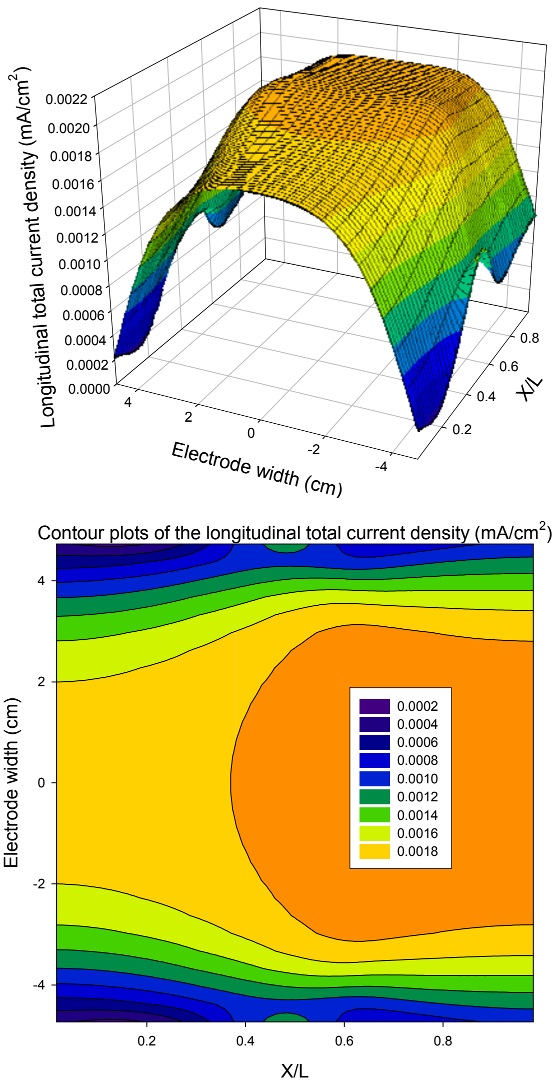

Fig. 3. Presentation in 2D and in contour plots of the longitudinal total current density in the stationary state

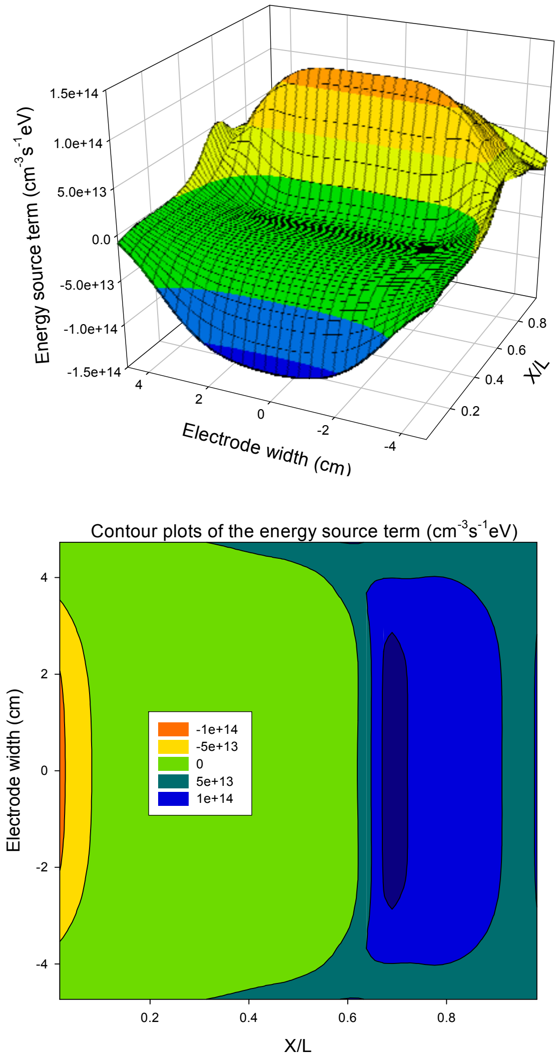

Fig. 4. Presentation in 2D and in contour plots of the energy source term in the stationary state

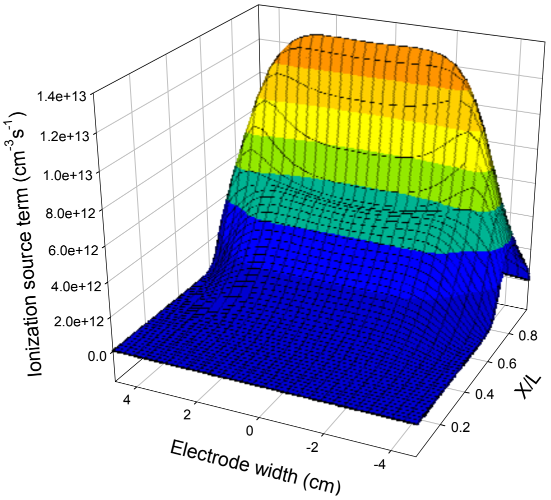

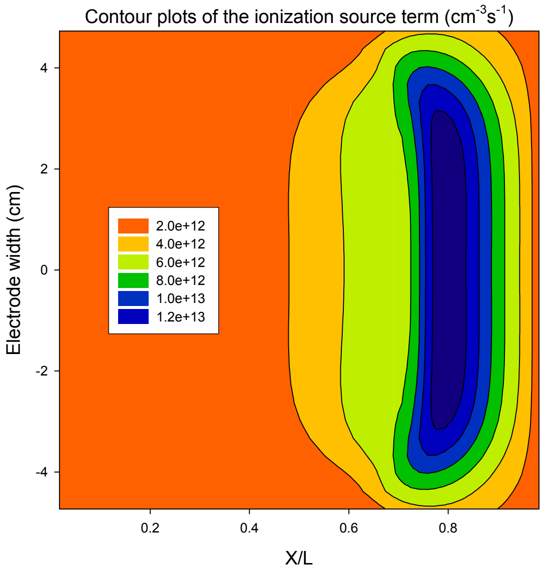

Fig. 5. Presentation in 2D and in contour plots of the ionization source term in the stationary state

Validity of the model

I investigated this discharge of the same conditions of both charged particles transports and geometry parameters as Lin *et al.*[16] To validate my results; I compared those issues on the symmetric axis of the electrodes with have been given by Lin *et al*[16] in the Figure 6.

I observe that the longitudinal current densities of electron, ion and total are in good agreement with those obtained by Lin et al.

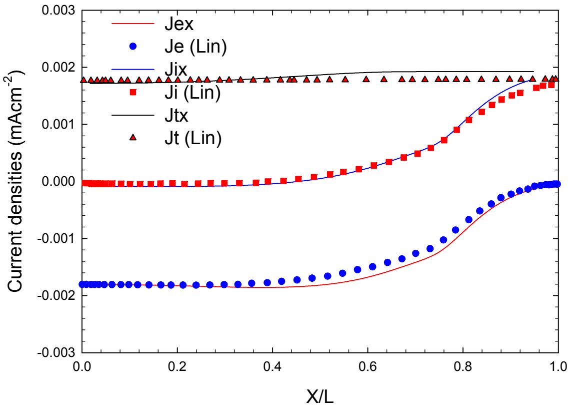

Fig. 6. Comparison between the spatial distributions of the longitudinal current densities of electron, ion and total in the stationary state on the symmetric axis of the electrodes and that given by Lin et al

Concluding remarks

In this article, a two-dimensional spatial distributions of the longitudinal current densities of electron, ion and total, and both ionization and energy sources terms have been presented in the stationary state of a DC normal glow discharge. Monatomic argon gas in low pressure has been utilized in this study. The discharge is maintained by a secondary electron emission coefficient at the cathode. The model used in this work is based on the first three moments of the Boltzmann's equation and the Poison's equation. The simulation results obtained were validated by using a comparative study with those of Lin et al.

Nomenclature

n_e , n_i	Electron and ion densities
$\boldsymbol{\Phi_e}$,$\boldsymbol{\Phi_i}$	Eelectron and ion fluxes
S	Net source term
μ_e , μ_i	Electron mobility, Ion mobility
D_e , D_i	Electron diffusivity, Ion diffusivity
K_i	Ionization rate prefactor
E_i	Ionization rate activation energy
T_e	Electron temperature
N	Gas density
K_B	Boltzmann's constant
E	Electric field.
ε_0	Permittivity of free space
e	Particle charge
ε_e	Electron energy
$\boldsymbol{\Phi_\varepsilon}$	Electron energy flux
H_i	Energy loss per ionizing collision

***Author**: Abdelaziz Bouchikhi was born in Tiaret, Algeria, on January,14,1973. He received the Doctor in 2010 at Oran-Algeria and habilitation in 2013 at SDB-Algeria. He is currently a Maitre Conference at University of Saida, Algeria.*
Email: bouchikhiabdelaziz1@yahoo.fr

REFERENCES

[1] Meyyappan M., Kreskovsky J. P., Glow discharge simulation through solutions to the moments of the Boltzmann transport equation, *J. Appl. Phys.*, (68)1990, No. 4, 1506-1512

[2] Bogaerts A., Gijbels R., Modeling of metastable argon atoms in a direct-current glow discharge, *Phys. Rev. A.*, (52)1995, No. 5, 3743-3751

[3] Bogaerts A., Gijbels R., Two-Dimensional Model of a Direct Current Glow Discharge: Description of the Argon Metastable Atoms, Sputtered Atoms, and Ions, *Anal. Chem.,* 68(1996), No.15, 2676-2685

[4] Schmitt W., Köhler W. E., Ruder H., A one-dimensional model of dc glow discharges, *J. Appl. Phys.*, (**7**1)1992, No. 12, 5783-5791

[5] Belenguer Ph., Boeuf J. P., Transition between different regimes of rf glow discharges, *Phys. Rev. A.*, (41)1990, No. 8, 4447-4459

[6] Oh Y. H., Choi N. H., Choi D. I., A numerical simulation of rf glow discharge containing an electronegative gas composition, *J. Appl. Phys.*, (6**7**) 1990, No. 7, 3264-3268

[7] Bouchikhi A., Hamid A., Through Solutions to the Moments of the Boltzmann Equation for DC Glow Discharge, *IRPHY.*, (2) 2008, No. 4, 196-203

[8] Bouchikhi A., Hamid A., One dimensional continuum model for dc glow discharge, *International Conference on Electrical Systems Design and Technologies*, Tunisia, 2008, www.iceedt.esgroups.org

[9] Bouchikhi A., Modèle fluide d'ordre deux en 1D et 2D d'une décharge luminescente, *Ph.D.* University of Oran, Algeria, 2010

[10] Bouchikhi A., Hamid A., 2D DC Subnormal Glow Discharge in Argon, *Plasma Sci. Technol.*, (12)2010, No. 1, 59-66

[11] Bouchikhi A., Two-dimensional numerical simulation of the DC glow discharge in the normal mode and with Einstein's relation of electron diffusivity, *Plasma Sci. Technol.*, 14(2012), No. 11, 965-973

[12] Marié D., Kutasi K., Malovié G., Donko Z., Petrovié Z. L., Axial emission profiles and apparent secondary electron yield in abnormal glow discharges in argon, *Eur. Phys. J. D.*, 21(2002),73-81

[13] Donko Z., Hybrid model of a rectangular hollow cathode discharge, *Phys. Rev. E.*, 57(1998), No. 6, 7126-7137 [14] Lin Y. H., Adomaitis R. A., A global basis function approach to dc glow discharge simulation, *Technical research report, T.R. 81*, University of Maryland, USA, 1997

[15] Lin Y. H., From detailed simulation to model reduction: development of numerical tools for a plasma processing application, *Ph.D.* Institute for Systems Research, University Maryland, USA, 1999, www.isr.umd.edu

[16] Lin Y. H., Adomaitis R. A., A global basis function approach to dc glow discharge simulation, *Physics. Letters. A.*, 243(1998), 142-150

[17] Park S., Economou D. J., Analysis of low pressure rf glow discharges using a continuum model, *J. Appl. Phys.*, 68(1990), No. 1, 3904-3915

[18] Fiala A., Modélisation Numérique Bidimensionnelle d'une Décharge Luminescente à basse pression, *Ph.D.* University of Toulouse, France, 1995

[19] Scharfetter D. L., H. K. Gummel, Large-signal analysis of a silicon Read diode oscillator, *IEEE. Trans. Electron Devices.*, (16)1969, No. 1, 64-77